EFFECT OF "STEFAN" CURRENTS OF A SOLIDIFYING MELT ON THE PROCESS OF THERMAL CONVECTION

P. F. Zavgorodnii, I. L. Povkh, and G. M. Sevost'yanov

UDC 532.54+536.252/421

The calculated results, represented by graphs, show that in the initial period of solidification the motion of a melt is fully determined by the shrinkage at the front of crystallization. The effect develops more strongly at lower Grashof numbers and higher Stefan numbers. As the rate of solidification and the temperature gradient decrease the process of natural thermal convection develops in the liquid phase. The calculated results are compared with experiment.

It is known that the thermal convection of the liquid core of a crystallizing ingot has a considerable effect on the processes of formation of the ingot's macrostructure. To determine the velocities of convective motion of the melt the authors of [1] performed a series of experimental studies which confirmed the presence of mixing of the liquid core up until its complete crystallization. Theoretical studies [2, 3] carried out on the assumption of the identical density of the liquid and solid phases give analogous results. Under actual conditions the densities of liquid and solidifying melts differ, and therefore so-called "Stefan" currents, whose direction is determined by the ratio of densities of the two phases, develop at the front of crystallization.

The influence of the shrinkage effects on the nature of the thermal convection is studied in the report. A rectangular region of a vertical cross section containing a melt whose initial temperature T_0 is higher than the crystallization temperature is analyzed. At a time $t > 0$ the temperature of the walls of the cavity is abruptly reduced to the crystallization temperature of the melt. The solid phase forms from the cold boundaries by a quadratic law with the direction of motion toward the center of the cavity. It is assumed that the convective motion has an axial symmetry relative to the vertical axis $0\eta_2$, and the further study of the thermal convection parameters is carried out for a cavity bounded above, on the side, and below by the solidification fronts and by the axis of symmetry $0\eta_2$ (Fig. 1).

For the solution of the stated problem a system of Navier–Stokes, heat transfer, and continuity equations is written in dimensionless form:

$$\frac{1}{\mathrm{Pr}}\frac{\partial \bar{V}}{\partial \tau} + (\bar{V}\nabla)\bar{V} = -\nabla\pi + \Delta\bar{V} + \bar{l}_g \mathrm{Gr}\theta; \tag{1}$$

$$\frac{\partial \theta}{\partial \tau} + \mathrm{Pr}(\bar{V}\nabla)\theta = \Delta\theta; \tag{2}$$

$$\nabla\bar{V} = 0 \tag{3}$$

with the boundary conditions

$$\bar{V}|_{\tau=0} = 0 \tag{4}$$

$$\theta|_{\tau=0} = 1;$$

$$\theta|_{\eta_1=\varepsilon_1} = \theta|_{\eta_2=H} = \theta|_{\eta_3=\varepsilon_2} = \frac{d\theta}{d\eta_1}\Big|_{\eta_1=0} = 0; \tag{5}$$

Donetsk. Translated from Zhurnal Prikladnoi Mekhaniki i Tekhnicheskoi Fiziki, No. 2, pp. 125-130, March-April, 1975. Original article submitted May 15, 1974.

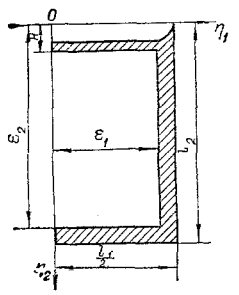

Fig. 1

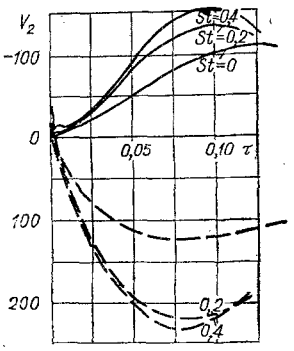

Fig. 2

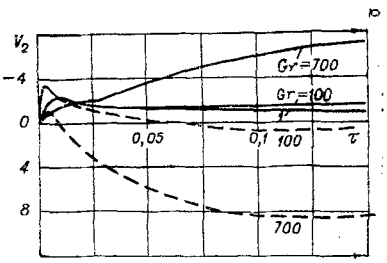

Fig. 3

$$V_1|_{\eta_1=0} = V_1|_{\eta_3=\varepsilon_3} = V_1|_{\eta_3=H} = V_2|_{\eta_1=\varepsilon_1} = \frac{dV_3}{d\eta_1}\Big|_{\eta_1=0} = 0; \tag{6}$$

$$V_3|_{\eta_3=\varepsilon_3} = -\mathrm{St}\varepsilon_3'; \quad V_1|_{\eta_1=\varepsilon_1} = -\mathrm{St}\varepsilon_1'; \tag{7}$$

$$V_3|_{\eta_3=H} = L_1, \tag{8}$$

where ε_i (i=1, 2, ...) is the relative width of the liquid zone; half the horizontal dimension of the cavity ($l_1/2$) is taken as the characteristic size; $\tau = t/t_0$ is the dimensionless time (Froude number); the characteristic time is $t_0 = l_1^2/4a$; a is the thermal diffusivity coefficient; L_1 is the rate of descent of the upper crust; $\mathrm{St} = (\rho_1/\rho_2 - 1)/\mathrm{Pr}$ is the Stefan number; ρ_1 and ρ_2 are the densities of the solid and liquid phases, respectively; ν is the coefficient of kinematic viscosity; $\theta = (T-T_C)/(T_0-T_C)$ is the dimensionless temperature; T_C is the crystallization temperature; T_0 is the initial temperature; $\mathrm{Pr} = \nu/a$ is the Prandtl number; $\mathrm{Gr} = g\beta(T_0-T_C)l_1^3/8\nu^2$ is the Grashof number; β is the temperature coefficient of volumetric expansion; $\pi = p/p_0$ is the dimensionless pressure; the sign ' denotes a derivative with respect to the time τ.

In the upper part of the ingot along with the formation of a solid crust there forms a shrinkage basin owing to the makeup of the side and lower solidification fronts with the melt. The equation of balance of the flow rates of the melt at the solid boundaries has the form

$$L_1\varepsilon_1 = [\mathrm{St}\varepsilon_1'(\varepsilon_3 - H) + \mathrm{St}\varepsilon_3'\varepsilon_1]. \tag{9}$$

Solving this equation for L_1 and substituting into (8), we obtain

$$V_3|_{\eta_3=H} = \mathrm{St}\left[\frac{\varepsilon_2 - H}{\varepsilon_1}\varepsilon_1' + \varepsilon_2'\right]. \tag{10}$$

Let us introduce the stream function ψ, connected with the velocity components V_1 and V_3 by the equations

$$V_1 = \frac{\partial\psi}{\partial\eta_2} \text{ and } V_2 = -\frac{\partial\psi}{\partial\eta_1},$$

the vorticity $\overline{\varphi} = \mathrm{rot}\,\bar{\mathbf{V}}$, and the time-dependent variables

$$\zeta_1 = \frac{\eta_1}{\varepsilon_1}, \quad \zeta_3 = \frac{\eta_2 - H}{\varepsilon_2 - H}, \tag{11}$$

which map a rectangular field with moving boundaries onto the unit field of a square. The system of equations (1)-(3) now takes the form

$$\frac{\partial\varphi}{\partial\tau} + \frac{1}{\varepsilon_1}\left[\frac{\mathrm{Pr}}{(\varepsilon_3 - H)}\frac{\partial\psi}{\partial\zeta_3} - \zeta_1\varepsilon_1'\right]\frac{\partial\varphi}{\partial\zeta_1} - \frac{1}{(\varepsilon_3 - H)}\left[\frac{\mathrm{Pr}}{\varepsilon_1}\frac{\partial\varphi}{\partial\zeta_1} + \zeta_3(\varepsilon_3' - H) + H'\right]\frac{\partial\varphi}{\partial\zeta_3} = \mathrm{Pr}\Delta_1\varphi - \frac{\mathrm{R}}{\varepsilon_1}\frac{\partial\theta}{\partial\zeta_1}; \tag{12}$$

$$\frac{\partial\theta}{\partial\tau} + \frac{1}{\varepsilon_1}\left[\frac{\mathrm{Pr}}{(\varepsilon_2 - H)}\frac{\partial\psi}{\partial\zeta_2} - \zeta_1\varepsilon_1'\right]\frac{\partial\theta}{\partial\zeta_1} - \frac{1}{\varepsilon_3 - H}\left[\frac{\mathrm{Pr}}{\varepsilon_1}\frac{\partial\psi}{\partial\zeta_1} + \zeta_3(\varepsilon_3' - H') + H'\right]\frac{\partial\theta}{\partial\zeta_3} = \Delta_1\theta; \tag{13}$$

$$\Delta\psi = -\varphi, \tag{14}$$

where

$$\Delta_1 = \frac{1}{\varepsilon_1^2}\frac{\partial^2}{\partial\zeta_1^2} + \frac{1}{(\varepsilon_3 - H)^2}\frac{\partial^2}{\partial\zeta_3^2}.$$

A coordinate grid and a time grid are introduced for the representation of system (12)-(14) in finite-difference form:

$$\omega_h = \{\zeta_1 = ih;\ \zeta_3 = mh;\ h = 1/I = 1/M;\ i = 1, 2, \ldots I;\ m = 1, 2 \ldots M\};$$

$$\tau_n = \left\{\tau = \sum_n n\tau_{x_1}\tau_k = A\frac{h_2}{4};\ 0 < A \leqslant 1;\ n = 1, 2 \ldots\right\}.$$

If one uses the method of fractional steps then Eqs. (12) and (13) after division along the coordinate axes $0\xi_1$ and $0\xi_3$ are written in the form

$$\frac{\varphi^{\wedge}_{i,m}-\varphi^{-}}{0.5\tau_k}=\frac{1}{\varepsilon_1}\left[ih\varepsilon_1'+\frac{\mathrm{Pr}}{(\varepsilon_2-H)}\left(\frac{\partial\psi}{\partial\zeta_2}\right)^{-}_{i,m}\right]\left(\frac{\partial\varphi}{\partial\zeta_1}\right)^{\wedge}_{i,m}+\frac{\mathrm{Pr}}{\varepsilon_1^2}\left(\frac{\partial^2\varphi}{\partial\zeta^2}\right)_{i,m}-\frac{\mathrm{R}}{2\varepsilon_1}\left(\frac{\partial\theta}{\partial\zeta_1}\right)^{-}_{i,m}; \tag{15}$$

$$\frac{\varphi^{+}_{i,m}-\varphi^{\wedge}_{i,m}}{\tau_k}=\frac{1}{(\varepsilon_3-H)}\left[mh\,(\varepsilon_3'-H)+H'+\frac{\mathrm{Pr}}{\varepsilon_1}\left(\frac{\partial\psi}{\partial\zeta_1}\right)^{-}\right]\left(\frac{\partial\varphi}{\partial\zeta_3}\right)^{+}+\frac{\mathrm{Pr}}{(\varepsilon_3-H)^2}\left(\frac{\partial^2\varphi}{\partial\zeta_3^2}\right)^{+}_{i,m}-\frac{\mathrm{R}}{2\varepsilon_1}\left(\frac{\partial\theta}{\partial\zeta_1}\right)^{-}_{i,m}; \tag{16}$$

$$\frac{\theta^{\wedge}_{i,m}-\theta^{-}_{i,m}}{0.5\tau_k}=\frac{1}{\varepsilon_1}\left[ih\varepsilon_1'+\frac{\mathrm{Pr}}{(\varepsilon_2-H)}\left(\frac{\partial\psi}{\partial\zeta_3}\right)^{+}_{i,m}\right]\left(\frac{\partial\theta}{\partial\zeta_1}\right)^{\wedge}_{i,m}+\frac{1}{\varepsilon_1^2}\left(\frac{\partial^2\theta}{\partial\zeta_1^2}\right)^{\wedge}; \tag{17}$$

$$\frac{\theta^{+}_{i,m}-\theta^{\wedge}}{\tau_k}=\frac{1}{(\varepsilon_3-H)}\left[mh\,(\varepsilon_3'-H')+H'+\frac{\mathrm{Pr}}{\varepsilon_1}\left(\frac{\partial\psi}{\partial\zeta_1}\right)^{+}_{i,m}\right]\left(\frac{\partial\theta}{\partial\zeta_3}\right)^{+}+\frac{1}{(\varepsilon_3-H)^2}\left(\frac{\partial^2\theta}{\partial\zeta_3^2}\right). \tag{18}$$

The Poisson equation in a form suitable for iteration is written as

$$\psi^{s+1}_{i,m}=\psi^{s}_{i,m}+\omega_0\left\{\frac{1}{2\left[\varepsilon_1^2+(\varepsilon_2-H)^2\right]}\left[(\varepsilon_3-H)^2\left(\psi^{s+1}_{i-1,m}+\right.\right.\right.$$

$$\left.\left.\left.+\psi^{3}_{i+1,m}\right)+\varepsilon_1^2\left(\psi^{s+1}_{i,m-1}+\psi^{s}_{i,m+1}\right)+\varepsilon_1^2(\varepsilon_3-H)^2h^2\varphi_{i,m}\right]-\psi^{s}_{i,m}\right\}, \tag{19}$$

where ω_0 is a relaxation parameter determined by the expression $\omega_0=2/(1+\sin\pi h)$; s is the number of the iteration.

In Eqs. (15)-(18) the symbols $-$, $\wedge$, and $+$ correspond to the n-th $(n+1/2)$-th, and $(n+1)$-th time layers.

From the condition (4) we obtain

$$\psi|_{\tau=a}=\varphi|_{\tau=a}=0;\quad \theta_{\tau=a}=1. \tag{20}$$

Expanding the temperature function in the vicinity of the boundary $\zeta_1=0$ with allowance for the condition (5) and Eq. (17), we obtain

$$\theta^{\wedge}_{0,m}=\frac{2\tau_k}{h^2+2\tau_k}\left[\theta^{\wedge}_{i,m}+\frac{h^2}{2\tau_k}\theta^{-}_{0,m}\right]. \tag{21}$$

The other temperature boundary conditions are satisfied exactly. For the determination of the boundary condition for the stream function at $\zeta_3=0$ the expression (10) is written in the form

$$-\frac{1}{\varepsilon_1}\frac{\partial\psi}{\partial\zeta}\Big|_{\zeta_3=0}=\mathrm{St}\left[\frac{\varepsilon_3-H}{\varepsilon_1}\varepsilon_1'+\varepsilon_2'\right].$$

Integrating the equation obtained along the coordinate ζ_1 and taking the integration constant as equal to zero, we obtain

$$\psi_{i,0}=-\mathrm{St}\left[\frac{\varepsilon_3-H}{\varepsilon_1}\varepsilon_1'+\varepsilon_2'\right]\varepsilon_1 ih. \tag{22}$$

The stream functions at the other boundaries are obtained analogously:

$$\psi_{0,m}=0;\ \psi_{i,M}=\mathrm{St}\,\varepsilon_3' ih; \tag{23}$$

$$\psi_{I,m}=-\mathrm{St}\,\varepsilon_1'(\varepsilon_3-H)\,mh. \tag{24}$$

The boundary conditions for the vorticity φ are obtained through expansion of the stream function at the corresponding boundaries using the conditions (6), (22)-(24), and the Poisson equation (14):

$$\varphi_{0,m}=0;\varphi_{i,m}=\frac{2}{h^2}(\mathrm{St}\,\varepsilon_3'\varepsilon_1 ih-\psi_{i,M-1}); \tag{25}$$

$$\varphi_{i,0}=-\frac{2}{h^2}\left\{\left[\mathrm{St}\left(\frac{\varepsilon_3-H}{\varepsilon_1}\varepsilon_1'+\varepsilon_2'\right)\right]\varepsilon_1 i+\psi_{i,1}\right\}; \tag{26}$$

$$\varphi_{I,m}=-\frac{2}{h^2}[\mathrm{St}\,\varepsilon_1'(\varepsilon_3-H)\,mh+\psi_{I-1,m}]. \tag{27}$$

Thus, the problem (15)-(19) with the boundary conditions (20)-(27) is formulated in finite-difference form. The integro-interpolation method developed in [4] was chosen for its numerical realization on a Dnepr-21 computer. The trial-run equations and the coefficients for them were determined in accordance with the same work. A cavity with a relative height $l_2=4$ was chosen for the study. The Prandtl number in all cases remained constant and equal to 0.224.

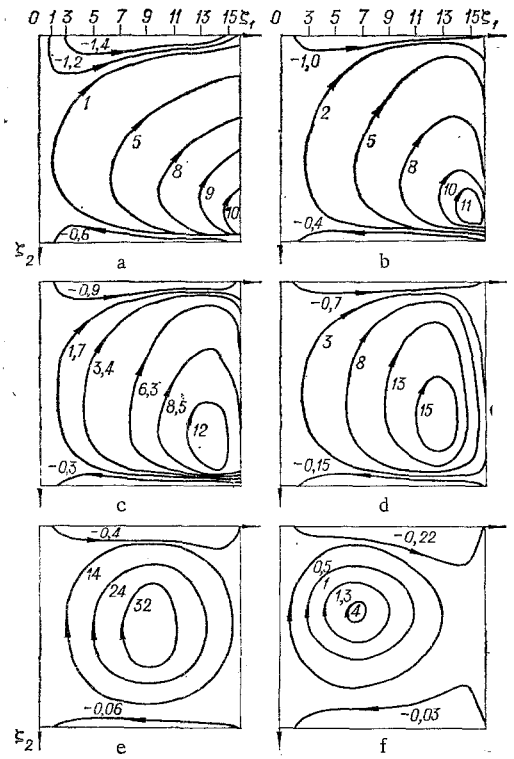

Fig. 4

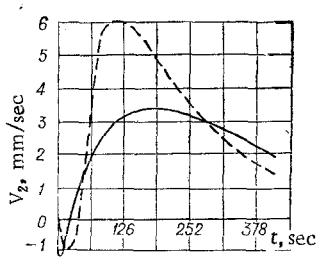

Fig. 5

As shown by the results of the calculation, presented in Fig. 2 (the solid lines are ascending currents and the dashed lines are descending currents), the development of thermal convection with time can be divided arbitrarily into three stages. The movement of the melt into the upper part of the cavity is observed near the solidification front in the interval of numbers $0 < \tau \leq \tau_1$. The duration of this stage and the maximum velocities in this interval essentially depend on the values of the Stefan numbers which characterize the degree of shrinkage of the solid phase. In the absence of shrinkage such properties do not develop in the liquid region (Fig. 2, curve 0).

With a decrease in the rate of growth of the solid crust the second stage, the stage of natural thermal convection, develops in the liquid part of the ingot under the effect of the temperature gradient. Acceleration of the convective motion occurs in the interval of Froude numbers $\tau_1 \leq \tau \leq \tau_2$, with the maximum velocity being reached at the end of this interval. As the results of the calculation show, an increase in the shrinkage of the solid phase causes an increase in the intensity of mixing of the melt with a concurrent decrease in the acceleration stage.

The third stage of the process ($\tau > \tau_2$) is characterized by a decrease in the intensity of mixing of the melt as its temperature decreases and by a transition to a mode of "creeping" flow.

The effect of the Grashof numbers on the process of thermal convection is illustrated by Fig. 3 (St = 0.2; the solid lines are ascending currents; the dashed lines are descending currents), from which it is seen that at small Grashof numbers (Gr = 1) the motion of the melt is determined only by the shrinkage effects at the boundaries of the solid phase. With an increase in the Grashof number the force of convective motion ($Gr\theta$) becomes the determining force in the process of development of the convective motion. The increase in the intensity of thermal convection is accompanied by a change in the duration of all the stages.

The calculated isolines of the stream function, the analysis of which allows one to trace the dynamics of the development of thermal convection, are plotted for an understanding of the hydrodynamic processes arising in the crystallizing liquid cores (Fig. 4, St = 0.5; a, b, c, d, e, f for τ = 0.03, 0.06, 0.02, 0.01, 0.09, and 0.19, respectively).

A characteristic property of these cases is the presence in the liquid phase of three independent zones closed at the boundaries of the solid phase at the starting time. Subsequently, vorticity starts to form in the lower corner of the cavity (see Fig. 4b) which is then "washed out" from the boundary by the melt descending at the solidificationfront (see Fig. 4c, d). The symmetrical location of the vortex (see Fig. 4e) corresponds to the maximum velocity in Fig. 2. As the cooled layers of the melt descend to the bottom part of the cavity the vorticity is displaced to the region of higher temperatures.

In Fig. 5 we present a comparison of the experimental (dashed line) and calculated (solid line) velocity component V_2 for $Gr = 0.5 \cdot 10^5$, Pr = 8.8, and St = 0.1. The experiment was performed on naphthalene by the method of [5]. The initial stage of thermal convection was recorded by continuous motion picture photography. The relative height of the mold was $l_3 = 4$ and the characteristic size was $l_1/2 = 30$ mm.

The analysis shows that the calculation and the experiment give qualitatively the same picture. The quantitative differences must be ascribed to the three-dimensionality of the experimental mold and the large amount of gas dissolved in the naphthalene which, being released from the solidified phase, promoted the formation of countermotion in the liquid phase.

Thus, the "Stefan" currents at the phase interface have an important effect on the intensity of convective motion. The effect is the more marked, the smaller the Grashof number and the greater the shrinkage.

LITERATURE CITED

1. V. A. Efimov et al., in: Steel Ingot Problems [in Russian], No. 4, Metallurgiya, Moscow (1969), pp. 93-95.
2. Yu. A. Samoilovich, Izv. Akad. Nauk SSSR, Metally, No. 2, 84-92 (1969).
3. É. A. Iodko, P. F. Zavgorodnii, and G. M. Sevost'yanov, Izv. Akad. Nauk SSSR, Teplofiz. Vys. Temp., 9, No. 5, 975-979 (1971).
4. A. A. Samarksii, Introduction to the Theory of Difference Systems [in Russian], Nauka, Moscow (1971).
5. É. A. Iodko et al., Izv. Akad. Nauk SSSR, Metally, No. 2, 102-108 (1971).